

Double-well magnetic trap for Bose-Einstein condensates

N. R. Thomas and A. C. Wilson

Physics Department, University of Otago, P.O. Box 56, Dunedin, New Zealand

C. J. Foot

Clarendon Laboratory, Department of Physics, University of Oxford, Parks Road, Oxford, OX1 3PU, United Kingdom

(Received 9 August 2001; revised manuscript received 5 March 2002; published 6 June 2002)

We present a magnetic trapping scheme for neutral atoms based on a hybrid of Ioffe-Pritchard and time-averaged orbiting potential traps. The resulting double-well magnetic potential has readily controllable barrier height and well separation. This offers a new tool for studying the behavior of Bose condensates in double-well potentials, and in particular for atom optics and interferometry. We formulate a description for the potential of this magnetic trap and discuss practical issues such as loading with atoms, evaporative cooling and manipulating the potential.

DOI: 10.1103/PhysRevA.65.063406

PACS number(s): 32.80.Pj, 03.75.Fi, 39.25.+k, 85.70.Ay

Bose-Einstein condensates (BECs) of dilute alkali-metal gases have been the subject of a great deal of attention since they were first realized [1–3]. Early experiments [4,5] used traps that were single harmonic wells, but recent interest has been focused on more complicated geometries. The simplest extension is the double-well trap, reported in Ref. [6] where a cigar-shaped condensate was split in half by a light sheet. When the BECs were released from this configuration, matter-wave interference was observed in an analog of Young’s double-slit experiment. In an extension of this experiment, vortices in one of the condensates were detected by observing a characteristic pattern in the interference [7]. Double wells have been theoretically studied in the context of combining two condensates [8,9], investigating phase fluctuations [10], detection of weak forces [11], Josephson junctions [12–17], and splitting a condensate [18–22]. Multiple-well traps have been created in a number of recent experiments using optical lattices, where several hundred wells may be occupied. There have been reports in the one– [23–29], two– [30,31] and three–dimensional [32] cases. These lattices are well suited to tunneling studies because the well spacing is submicron.

In this paper we describe a trap in the simpler double-well configuration. It relies on magnetic fields only, avoiding the need to mechanically stabilize the magnetic field with respect to an optical one. The trap has a well separation that can be large, up to several centimeters, allowing good optical access to each condensate. Our scheme is an extension of the existing Ioffe-Pritchard (IP) and time-averaged orbiting potential (TOP) traps used in many BEC experiments. We begin by briefly summarizing the IP trap and review how a double-quadrupole-like potential can be formed. Bose condensates cannot be confined in this potential, because of Majorana spin-flip loss, but we show how the addition of a rotating bias field can resolve this problem. The focus of this work is on the development of a theoretical description of the resulting double-well magnetic potential. Practical issues such as the effect of gravity, loading atoms, evaporative cooling, and controlling the shape of the potential are considered in detail.

I. IOFFE-PRITCHARD TRAPS

IP traps [33,34] have been used extensively in the realization of BEC in alkali gases. The basic configuration for an IP trap is illustrated in Fig. 1. Four long “bars” with currents in alternate directions run parallel to the z axis. These generate a quadrupole field in the x - y plane with gradient B' , which leads to radial confinement. Two “pinch” coils have currents in the same direction and are spaced to give a harmonic local minimum of the axial magnetic field with curvature B'' . These coils provide axial confinement but also a large bias field B_p . Finally there are the two “nulling” coils (usually in the Helmholtz configuration) that provide a uniform axial field B_n . These allow the total bias field at the trap center,

$$B_o = B_p - B_n, \quad (1)$$

to be reduced. For BEC experiments this is important because it leads to tighter radial confinement and simplifies rf evaporation [35].

The magnetic field components for this geometry, to second order about the trap center, are given by the equations

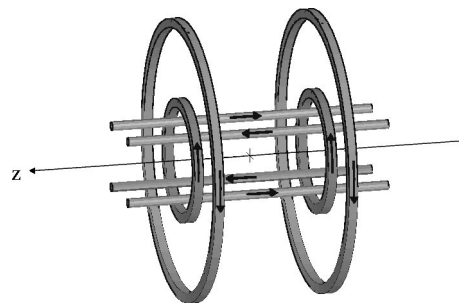


FIG. 1. The layout of coils and bars for a Ioffe-Pritchard magnetic trap with current direction indicated by arrows. The four bars lie on corners of a square. Current in each bar flows in the direction opposite to that of its closest neighbors, and the magnitude of the current is the same for each bar. The two pairs of coils with large and small radii are the nulling and pinch coils, respectively. The currents flow in the opposite sense so that they produce opposing magnetic fields.

TABLE I. A summary of reported IP trap parameters. In many cases the traditional geometry of Fig. 1 is replaced by a variant with some specific advantages.

Ref.	Variant	Species	B_o (G)	B' (G/cm)	B'' (G/cm ²)
[36]	Cloverleaf	²³ Na	1	170	125
[37]	Baseball	⁸⁷ Rb	1.6	300	85
[38] ^{a,b}	Perm. Magnet	⁷ Li	1000	1250	855
[39] ^a	Four-Dee	²³ Na	1.5	220	240
[40]	Traditional	⁸⁷ Rb	1.5	275	365
[41]	QUIC	⁸⁷ Rb	2	220	260
[42]	Three-coil	⁸⁷ Rb	1.3	140	85
[43]	Superconductor	H	0.5	240	0.75
[44] ^a	Perm. Magnet	⁸⁷ Rb	190	1200	400
[45]	Cloverleaf	²³ Na	1	330	200
[46] ^a	Baseball	⁸⁷ Rb	1	175	62
[47]	Cloverleaf	⁸⁷ Rb	1	175	185
[48] ^a	QUIC	⁸⁷ Rb	1.6	170	110
[49] ^a	Cloverleaf	⁴ He*	0.3	85	40
[50]	QUIC	⁴ He*	4.2	280	200

^aField quantities calculated from trap oscillation frequencies.

^bEquivalent radial gradient for traps that are harmonic.

$$\begin{aligned}
 B_x &= +B'x - \frac{1}{2}B''xz, \\
 B_y &= -B'y - \frac{1}{2}B''yz, \\
 B_z &= B_o + \frac{1}{2}B''\left(z^2 - \frac{1}{2}r^2\right),
 \end{aligned} \tag{2}$$

where r is the radial coordinate ($r^2 = x^2 + y^2$). The terms with coefficient B' are generated by the four bars. Atoms in a weak-field seeking state are trapped at the minimum of the field magnitude. For small thermal atomic clouds and Bose-Einstein condensates ($k_B T < \mu B_o$), the field magnitude is calculated by a binomial expansion to second order, to give

$$B_{\text{IP}} = B_o + \frac{1}{2}\left(\frac{B'^2}{B_o} - \frac{B''}{2}\right)r^2 + \frac{1}{2}B''z^2, \tag{3}$$

where $B_o > 0$. The radial curvature is large when $B'^2/B_o \gg B''/2$, which is achieved by reducing B_o with the nulling coils. A summary of reported parameters for various IP traps used in BEC experiments is shown in Table I. Typical values for the popular coil-based IP traps are $B_o = 1$ G, $B' = 200$ G/cm, and $B'' = 150$ G/cm². Note that the curvature is usually much larger radially than axially so that atomic clouds are *cigar* shaped with their long axis in the z direction. For the values above, the radial curvature is $B''_r \approx 40\,000$ G/cm² and the anisotropy is $\lambda \equiv \omega_r/\omega_z = \sqrt{B''_r/B''_z} = 16.3$. In this calculation ω_z and ω_r are the axial and radial oscillation frequencies in the harmonic trap.

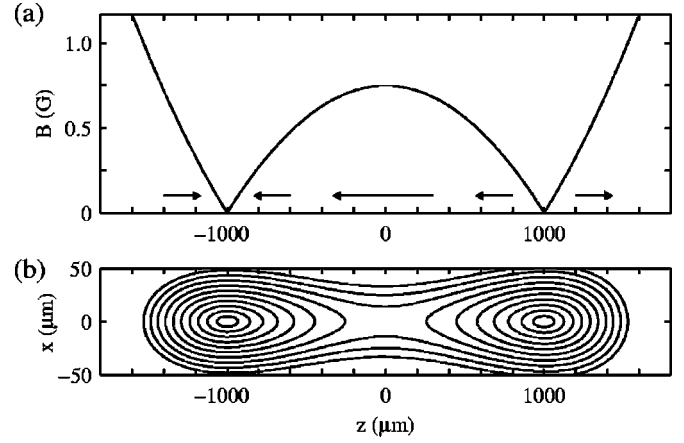


FIG. 2. A double-well potential with well spacing of $2z_o = 2$ mm, generated by fields of $B_o = -0.75$ G, $B' = 200$ G/cm, and $B'' = 150$ G/cm². (a) The behavior for the z axis with the field directions indicated by arrows. (b) Field magnitude contours in the x - z plane with 0.1 G spacing. The barrier height is equivalent to a temperature ($= \mu \Delta B/k_B$) of 50 μ K for atoms in a magnetic substate with $\mu = \mu_B$.

Ketterle *et al.* [5,51] have pointed out that a double-well is formed if the nulling bias (B_n) is allowed to overcome the pinch bias (B_p), so that $B_o < 0$ in Eq. (1). The axial field now has zeros at the points $z_{\pm} = \pm z_o$, where

$$z_o = \sqrt{\frac{2|B_o|}{B''}}. \tag{4}$$

The trapping potential then has the form of two wells, as shown in Fig. 2. The barrier height ΔB is $|B_o|$, which occurs at $(z, r) = (0, 0)$.

The field components, from Eq. (2) evaluated about the well minima z_{\pm} , are given by

$$\begin{aligned}
 B_x &= \left(+B' - \frac{1}{2}B''z_{\pm}\right)x, \\
 B_y &= \left(-B' - \frac{1}{2}B''z_{\pm}\right)y, \\
 B_z &= B''z_{\pm}z' + \frac{1}{2}B''z'^2,
 \end{aligned} \tag{5}$$

where $z' = z - z_{\pm}$. If we were to neglect the term in z'^2 , then these equations would be similar to those of a spherical quadrupole field. This approximation is reasonable near the bottom of each well, where $|z'/2z_o| \ll 1$. However, in general, the curvature distorts the potential from a quadrupole. Note that the axial gradient scales with the well position z_o , so that confinement tightens and becomes more linear as the well separation increases. The gradients along the x and y axes are very similar because we will consider well separations small enough that $B' \gg B''z_o$. The x - y asymmetry is therefore small and can often be neglected, but we include it in subsequent calculations for completeness.

The usefulness of the potential in Fig. 2 for BECs is severely limited by Majorana spin flips at the two field zeros

[52,53]. Removing this means of trap loss from the double-well trap is the motivation behind this work.

II. DOUBLE-TOP TRAP

To eliminate loss from the two quadrupolelike wells, we apply the TOP trap scheme developed by Cornell and co-workers for the simple quadrupole trap [52], that is, we add a rotating bias field to the double-well IP trap. The rotating field component, with magnitude B_t , is chosen to be

$$\begin{aligned} B_x &= B_t \cos \omega t, \\ B_y &= B_t \sin \omega t, \\ B_z &= 0. \end{aligned} \quad (6)$$

The oscillating field has no z component, which avoids the introduction of further radial asymmetry and modulation of the well spacing, stiffness, and barrier height during the bias rotation. This choice also leads to a relatively simple description of the trap. As in the standard TOP trap, the frequency of rotation ω must satisfy

$$\omega_z, \omega_r \ll \omega \ll \omega_L, \quad (7)$$

where ω_L is the Larmor frequency in field B_t . The lower bound ensures a time-averaged potential, and the upper bound allows the atomic magnetic dipole to follow the oscillating field so that the atoms remain trapped. These limits cause no practical difficulties as trap oscillation and Larmor frequencies are normally of order 100 Hz and 1 MHz, respectively.

The key mechanism of the TOP trap is that the field zero of a spherical quadrupole is displaced outside the atomic cloud by the rotating bias field of Eq. (6). In the original implementation [52] the field rotated about the symmetry axis of a spherical quadrupole giving a circular locus of $B = 0$ at radius $r_o = B_t/B'$, where B' is the radial gradient of the quadrupole. The double-TOP trap described in this work does not in general have equal gradients in the plane in which the bias rotates, so the locus is slightly elliptical. The axial displacements for x and y are given by

$$r_i = \frac{B_t}{|B'_i|}, \quad (8)$$

where $i = \{x, y\}$ and $B'_i = \partial B_i / \partial i$ is the magnetic field gradient on axis i evaluated from Eq. (5). Some other implementations of the TOP trap [54,55] also have an elliptical locus because the oscillating magnetic field does not rotate about the symmetry axis of a spherical quadrupole. The double-TOP will have a circular locus for the field zeros when the x - y asymmetry is negligible, corresponding to the limit $z_o \ll 1$ cm for our typical parameters.

Following Cornell's method for the standard TOP trap, the field distribution for the double-TOP can be evaluated by averaging the field magnitude,

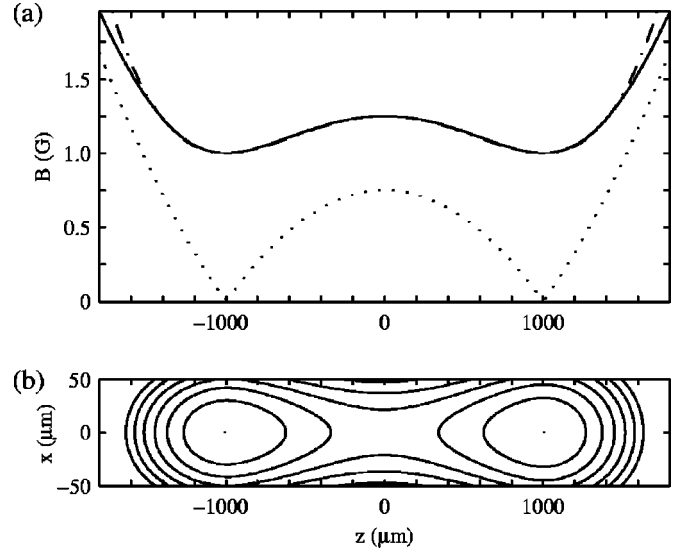


FIG. 3. A double-TOP potential with the same parameters as Fig. 2 ($2z_o = 2$ mm, $B_o = -0.75$ G), and $B_t = 1$ G. (a) The behavior on the z axis with numerical (solid), Mexican-hat (dash-dot), and double-well IP (dotted) potentials shown. (b) A contour plot in the x - z plane for the numerical integration with 0.1 G spacing starting from the well bottom B_t . The barrier height is equivalent to 17 μK for atoms with $\mu = \mu_B$.

$$B_{\text{av}} = \frac{\omega}{2\pi} \int_0^{2\pi/\omega} B(t) dt, \quad (9)$$

where $B(t)$ is the instantaneous field magnitude. In Fig. 3 we have numerically evaluated Eq. (9). The addition of the rotating bias field to the double-well IP trap has displaced the field zero as required, leaving a minimum of field magnitude of B_t occurring at $(z, r) = (z_{\pm}, 0)$. The field at the top of the barrier separating the two wells is now the quadrature sum of static and rotating bias fields, given by

$$B_b = \sqrt{B_o^2 + B_t^2}. \quad (10)$$

The barrier height ΔB is then given by $\Delta B = B_b - B_t$. The well separation is not affected by the addition of the rotating bias field.

There is no straightforward analytical solution to Eq. (9) that applies for a wide range of parameters. However, it is possible to find results for restricted conditions and we now present two such cases. Along the central axis of the trap, the field magnitude can be approximated by a one-dimensional Mexican-hat functional form

$$B_{\text{av}}(z) = B_t + \Delta B \left[1 - \left(\frac{z}{z_o} \right)^2 \right]^2, \quad (11)$$

and the error is less than 1.5% for $|B_o|/B_t \leq 1$ in the region $|z|/z_o \leq \sqrt{2}$. This description becomes more accurate as the ratio $|B_o|/B_t$ becomes smaller. Figure 3 shows that the fit is best in the central region where $B_t \leq B_{\text{av}}(z) \leq B_b$. At larger values of z the time-averaged field is dominated by the static axial component, so the potential becomes harmonic.

The second case is to consider the shape of each well near the minimum. This description applies to a cold atomic cloud confined within either well. We proceed by performing an

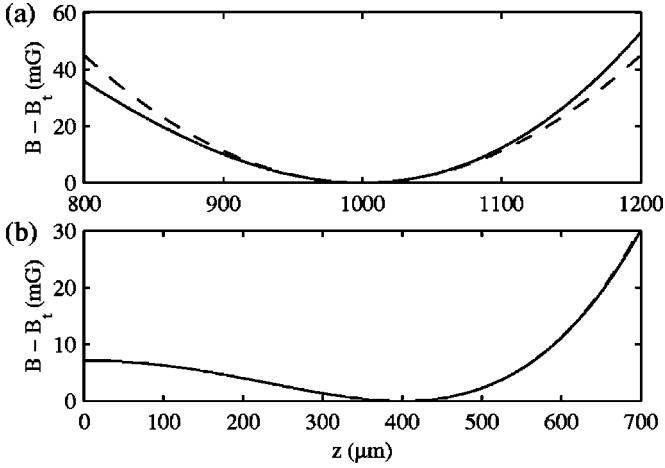


FIG. 4. Right-hand well of double-TOP potentials with common field parameters $B' = 200$ G/cm, $B'' = 150$ G/cm², and $B_t = 1$ G. Both the numerical average (solid) and evaluation of Eq. (12) (dashed) are shown. (a) The axial potential for widely separated wells ($z_o = 1000$ μm) and relatively high barrier ($\Delta B = 250$ mG). Equation (12) is evaluated to second order. (b) The axial potential for smaller well spacing ($z_o = 400$ μm) and a low barrier ($\Delta B = 7.2$ mG). The analytical result is taken to fourth order in z .

analytical integration of Eq. (9), using the double-well fields expanded about $z = \pm z_o$ and the rotating bias. The resulting field magnitude is given by

$$B_{av} = B_t + \frac{1}{2} \left(\frac{B'^2}{2B_t} + \frac{|B_o|B''}{4B_t} \right) r^2 + \frac{B''B'}{4B_t} z_{\pm} (y^2 - x^2) + \frac{|B_o|}{B_t} B'' z'^2 + \frac{B''^2}{2B_t} z_{\pm} z'^3 + \frac{B''^2}{8B_t} z'^4. \quad (12)$$

Examining this result we find that the radial dependence is harmonic and is dominated by the term $B'^2/(2B_t)$, which is identical to the standard TOP trap with field rotating in the x - y plane. The term in $(y^2 - x^2)$ is the result of the slight x - y asymmetry of the double well and is negligible for $z_o \ll 1$ cm. Compared to the single-well IP trap of Eq. (3) the axial curvature has been modified by the factor $2|B_o|/B_t$, so that axial confinement is tightened for $|B_o| \approx B_t$. The terms in z'^3 and z'^4 describe the barrier, and for our typical parameters these terms are important when z_o is smaller than approximately 500 μm . If the wells are more widely spaced, the third-order term adds only a slight tilt to the harmonic confinement and the fourth-order term can be neglected, as shown in Fig. 4.

We now consider the effect of gravity on the potential. In general, the center-of-mass position of an atomic cloud will sag in the magnetic potential to the point that the magnetic force is equal to the gravitational one. This has been considered in detail for an extremely weak TOP trap [56] and here we point out only the important features for the double-TOP. We take gravity in the $-x$ direction (downwards in Fig. 1). In the limit of insignificant x - y asymmetry the sag is given simply by

$$x_s = -\frac{mg}{\mu B''_x} \approx -\frac{mg}{\mu} \frac{2B_t}{B'^2}, \quad (13)$$

where m and μ are the atomic mass and magnetic moment, g is the acceleration due to gravity, and B''_x is the curvature of the field in the x direction. The displacement must be considerably smaller than the radius of the quadrupole zero rotation to prevent spin-flip loss (the size of the atomic cloud determines the required relative size). The ratio of these two quantities is approximated by

$$\frac{x_s}{r_x} \approx \frac{2mg}{\mu B'} \quad (14)$$

in the limit $B' \gg \sqrt{3/4|B_o|B''}$. This condition is weaker than that introduced in Sec. I for the x - y asymmetry, and is satisfied for the parameter values used in this paper. The ratio evaluates to an acceptable 0.15 for ^{87}Rb in the $|F=2, m_F=2\rangle$ state and $B' = 200$ G/cm.

Equation (13) is a useful approximation but in general even a modest x - y asymmetry should be considered, as it leads to a spatial variation in B''_x . The resulting difference in displacement and potential minima for the two wells is due to the interaction of the Ioffe bar quadrupole field and the curvature of the pinch field. This effect can be described by a gradient along the z axis, given by

$$-\frac{B''B'}{4B_t} \bar{x}_s^2 z \approx -\left(\frac{mg}{\mu}\right)^2 \frac{B''B_t}{B'^3} z, \quad (15)$$

where \bar{x}_s is the mean sag of the two wells, and is given by Eq. (13). For our example, the presence of gravity leads the left well minimum to sag 7.1 μm and 360 nK, while the right well sags 8.22 μm and 423 nK. These sags compare favorably to the original barrier height of 17 μK , and for many applications this effect of gravity is likely to be minimal. However, in the extreme case, the relative shift in the well minima will be larger than the original barrier height, which corresponds to

$$\left(\frac{mg}{\mu}\right)^2 \sqrt{\frac{8B_t^4 B''}{B'^6 |B_o|^3}} > 1. \quad (16)$$

In situations where symmetry is important, it can be restored by applying an opposing magnetic field gradient. In the later two sections of this paper we assume this correction.

In summary, the complete potential can be calculated numerically, while near the well minima can be described analytically. The Mexican-hat functional form is a useful approximation for the axial field magnitude in the central region. The effect of gravity can be an important consideration.

III. LOADING A CONDENSATE FROM A IOFFE-PRITCHARD TRAP

The double-TOP trap may be loaded with a Bose condensate by transfer from a IP trap. To do this without spin-flip loss, it is necessary to apply the rotating bias before reverse biasing to form a double well. We model this loading scheme by adding the rotating bias of Eq. (6) to the IP field compo-

nents of Eq. (2), and on integrating for the magnitude find that

$$B_{av} = B_b + \frac{1}{2} \left[\frac{B_o}{B_b} \left(\frac{B'^2}{B_o} - \frac{B''}{2} \right) - \frac{B_t^2 B'^2}{2B_b^3} \right] r^2 + B' B'' \frac{B_o^2 + B_b^2}{4B_b^3} z(y^2 - x^2) + \frac{1}{2} \frac{B_o}{B_b} B'' z^2 + \frac{B_t^2 B''^2}{8B_b^3} z^4. \quad (17)$$

Compared to the initial IP trap, both the axial and radial curvatures are reduced by at least a factor of B_o/B_b due to the time average. This effect can be minimized if $B_b \approx B_o$, which occurs when B_t is small in comparison to B_o . Since $B_o > 0$, there are no zeros of the field in this configuration and therefore there is no restriction on the minimum size of B_t . This choice of parameters also minimizes the effect of the third term in the radial curvature. A fourth-order term in z is required because the axial curvature goes to zero with B_o .

We consider the loading process as an adiabatic evolution from IP to the time-averaged IP trap and finally to double-TOP. We can use Eq. (17) to describe most of this process, as shown in Fig. 5. The first step is to increase B_t from 0 to 1 G while holding $B_o = 1$ G. The trap minimum becomes $B_b = \sqrt{2}B_o$, and the axial and radial curvatures are reduced by factors of 0.71 and 0.53, respectively. A typical condensate is sufficiently small ($\approx 150 \mu\text{m}$ long) for the axial confinement to be harmonic. The second stage is to ramp B_o down to -0.75 G which creates a double-TOP trap characterized by $\Delta B = 250$ mG, $2z_o = 2000 \mu\text{m}$. During this ramp the radial confinement is mostly unchanged because the rotating bias dominates B_b . When B_o passes through zero, B_t must be sufficiently large to place the field zero outside the cloud of atoms and prevent spin-flip loss. For the parameters used, the radial curvature of $20\,000 \text{ G/cm}^2$ at $B_o = 0$ means a typical alkali condensate of 10^6 atoms will be significantly inside $r_o = 50 \mu\text{m}$. The ramp of B_o produces a dramatic change in potential on the z axis. While $B_o > 0$, the curvature is positive but reducing, leading to a flattening as the quartic term becomes more important. Some control of the rate of change of the curvature is possible by the choice of B_t relative to B_o . In this case, where they are approximately equal at start of the ramp, the curvature does not greatly deviate from a linear reduction, and this is also true for the case $B_t > B_o$. In the opposite extreme the curvature can collapse quite suddenly. When B_o passes through zero, the sign of the curvature reverses and the barrier starts to rise. In Fig. 5(f) we see that although the analytical solution [Eq. (17)] describes the qualitative shape of the potential, there is no longer a good quantitative agreement with the numerical result. The Mexican-hat description is more appropriate for this situation.

A second method for loading Bose condensates into a double-TOP configuration is to evaporatively cool a thermal cloud. In this case the evaporation process is much the same as for a standard TOP trap, with the rf field oriented perpendicular to the rotating bias field, except that rf resonance

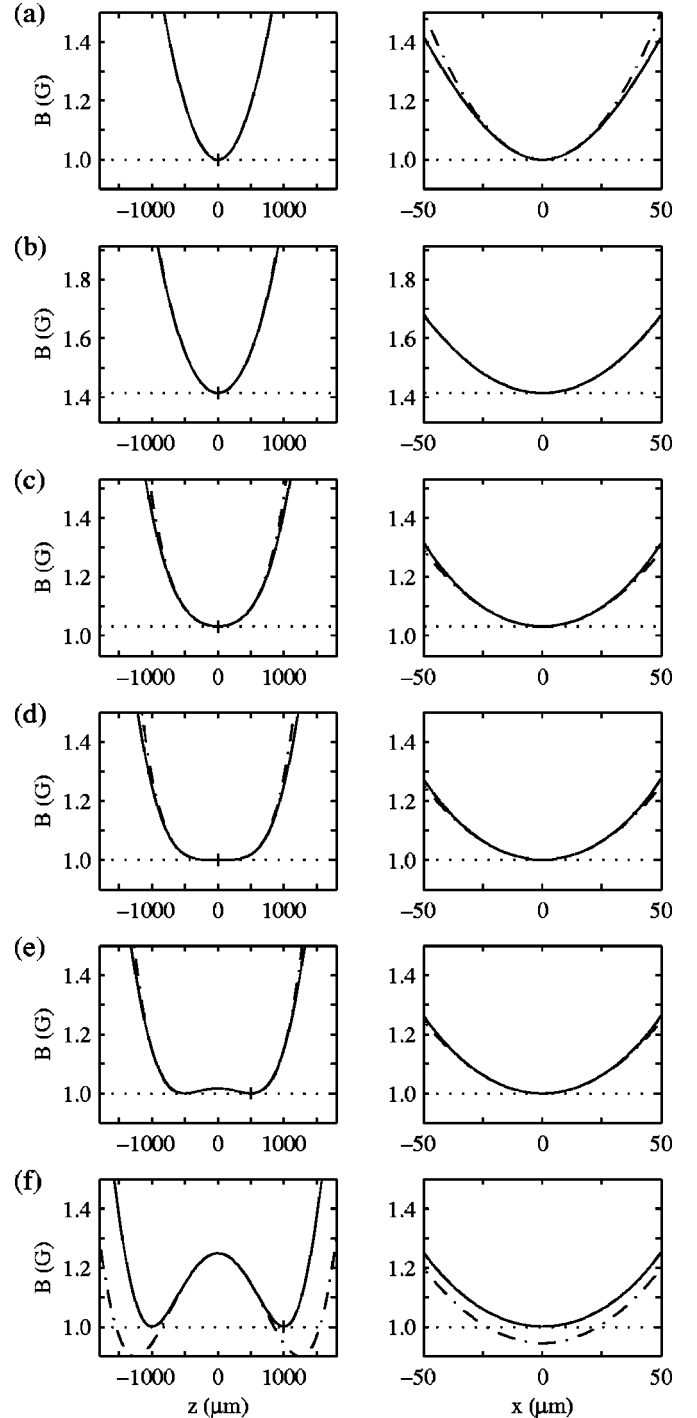


FIG. 5. Numerical (solid) and analytical (dash-dot) modeling of the transformation from IP to double-TOP trap by reducing B_o . The behavior is shown for the z axis (left column) and the x direction at the trap minima (right column) indicated by the marker on the corresponding z -axis plot. The plots show (a) the initial IP trap with $B_o = 1$ G, $B' = 200 \text{ G/cm}$, $B'' = 150 \text{ G/cm}^2$, $B_t = 0$ G; (b) the time-averaged IP formed with $B_t = 1$ G; (c)–(f) B_o equal to 0.25 G, 0 G, -0.19 G, and -0.75 G, respectively (all other parameters held constant). The well separations in (e) and (f) are $2z_o = 1000 \mu\text{m}$ and $2000 \mu\text{m}$. The radii of the locus traced by the two quadrupole field zeros in (d)–(f) are constant and equal to $r_x = 51.9 \mu\text{m}$ and $r_y = 48.2 \mu\text{m}$ for the right-hand well (vice versa for left well).

occurs at two points at the perimeter of the cloud rather than one. Alternatively, an atomic cloud could be cooled first in a IP trap and then in a double-TOP. However, in this case, the standard orientation for the rf antenna in a IP trap is not well matched for optimum evaporation in the double-TOP.

IV. CONTROLLING THE BARRIER HEIGHT AND WELL SPACING

In this section we consider changing the shape of the double-TOP potential over a range of conditions suited to experiments with Bose condensates. As above, we will keep the IP gradient and curvature constant and adjust the two bias fields B_o and B_t .

In the absence of external influences, the minimum spacing of the two wells is set by experimental noise on coil currents. Large currents (several hundred amps) are common for Ioffe-Pritchard traps, and the power supplies required often have modest stability. However, the compact quadrupole Ioffe configuration (QUIC) [41], which uses an extremely stable current and μ -metal shielding, has residual ac magnetic fields of less than 0.1 mG [57]. With comparable care in design one might expect similar stability from a double-TOP trap. For our typical parameters, a bias field B_o of 10 mG (100 times the residual field noise reported by Hänsch and co-workers) gives a well spacing of 230 μm . We regard this as a reasonable practical limit on the smallest possible well spacing. The upper bound on well spacing will be determined by vacuum system size and imaging considerations, but may be as large as several centimeters.

As discussed in Sec. II, the rotating bias field, B_t , must be large enough to place the locus of the quadrupole field zero outside the cloud. Further, it has been suggested [56] that B_t must be large enough that atoms in the bottom of the potential are not resonant with ac field noise, which will give rise to transitions to untrapped states. A rotating field magnitude of 1 G is commonly used in TOP traps, but smaller values are possible with greater attention to noise performance. The largest rotating bias field that has been reported for a TOP trap is 50 G [58]. It is important to note that large B_t relaxes the radial confinement, so that the effects of the trap x - y asymmetry and gravity must be accounted for. Combining a range of 1 G to 50 G for B_t with B_o between 10 mG and 1 G leads to barrier heights ($\mu_B \Delta B / k_B$) of 67 pK to 28 μK .

We now compare these heights to a condensate chemical potential μ_c , see Ref. [59]. For the trap parameters associated with Fig. 5(f) we have $\Delta B = 0.25$ G, or $\mu_B \Delta B / k_B = 16.8$ μK . The chemical potential, for 10^6 atoms of ^{87}Rb in the $|F=2, m_F=2\rangle$ state, confined in one of the wells is $\mu_c / k_B = 180$ nK, were we have approximated the well as harmonic. In this case, the ratio of barrier height to chemical potential is then $\mu_B \Delta B / \mu_c = 93$, so that the condensates are essentially isolated from each other. The relative barrier height may be brought closer to unity by one or both of the following methods: (a) lowering B_o (also reducing the well spacing), or (b) increasing B_t (also relaxing the radial confinement but leaving z_o unchanged). We plot both cases in Fig. 6. A numerical calculation of the chemical potential was used, where we integrated over the magnetic potential in the

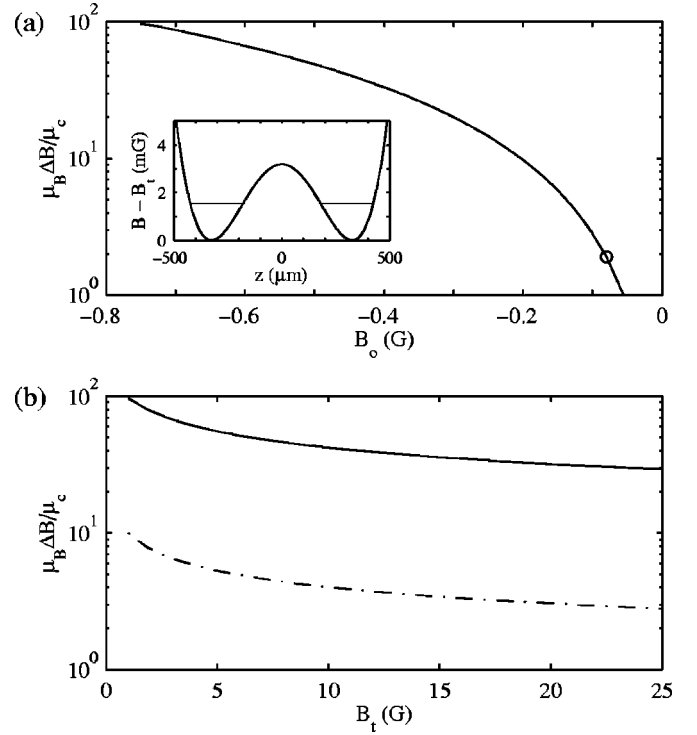


FIG. 6. (a) Control of the relative barrier height by altering the static bias field B_o with $B_t = 1$ G. In the range shown, the ratio of barrier height and chemical potential drops from 100 to 1. The circle indicates the parameters used for the inset. Inset: the magnetic potential for $B_o = -80$ mG and the chemical potential (horizontal lines) for 10^6 Rb atoms in each well. The calculation of μ_c neglects any effect of the condensate in the other well. (b) Control of the barrier height by altering the rotating bias field B_t with B_o equal to -0.75 G (solid) and -0.20 G (dash-dot).

Thomas-Fermi approximation. For each potential, we kept the number of atoms constant at 10^6 and solved for μ_c . By reducing the well separation the relative barrier height can be reduced by two orders of magnitude, with the condensate chemical potential equaling the barrier height at $B_o = -55$ mG. The scaling with the rotating bias field is weaker and therefore offers the possibility fine control for an appropriate choice of B_o .

Given the range of options for controlling the potential, the double-TOP trap is ideally suited to storage and manipulation of Bose condensates. An atom interferometer in which the condensates remain trapped could be realized. Also, since large well separations are readily achievable, a condensate in one well can be perturbed independent of the other.

Controlling the barrier height in a double-well trap raises the possibility of investigating Josephson tunneling. However, due to the double-TOP geometry, we do not expect that tunneling will be observable in this trap. It has been shown [17] that very small separations are required to overcome suppression of tunneling by the condensate mean field. Simple numerical calculations indicate that the tunneling rate in the double-TOP trap is immeasurably small.

V. CONCLUSIONS

We have developed a theoretical description of a double-well magnetic trap suitable for ultracold samples of neutral

atoms, and Bose condensates in particular. Analytical expressions describing the potential are derived and these are in good agreement with numerical simulations of the time-averaged field. We have outlined procedures for loading the double-TOP trap. In one case a Ioffe-Pritchard trap is used to form a condensate that is then transformed into a double-TOP. We also considered direct rf evaporation in a double-TOP potential. We have discussed changing the shape of the double-TOP potential over a range of conditions suited to experiments with Bose condensates. The separation of the

wells is controlled by the static bias field B_o , while the barrier height also depends on the rotating bias field B_r . The double-TOP trap is a hybrid of existing magnetic trapping technologies.

ACKNOWLEDGMENTS

We acknowledge the support of the Marsden Fund, Contract No. UOO910, and the University of Otago.

-
- [1] M. H. Anderson, J. R. Ensher, M. R. Matthews, C. E. Wieman, and E. A. Cornell, *Science* **269**, 198 (1995).
- [2] K. B. Davis, M.-O. Mewes, M. R. Andrews, N. J. van Druten, D. S. Durfee, D. M. Kurn, and W. Ketterle, *Phys. Rev. Lett.* **75**, 3969 (1995).
- [3] C. C. Bradley, C. A. Sackett, J. J. Tollett, and R. G. Hulet, *Phys. Rev. Lett.* **75**, 1687 (1995); **79**, 1170 (1997).
- [4] E. Cornell, J. Ensher, and C. Wieman, in *Proceedings of the International School of Physics—Enrico Fermi*, edited by M. Inguscio, S. Stringari, and C. Wieman (IOS Press, Amsterdam, 1999), p. 15.
- [5] W. Ketterle, D. S. Durfee, and D. M. Stamper-Kurn, in *Proceedings of the International School of Physics—Enrico Fermi* (Ref. [4]), p. 67.
- [6] M. R. Andrews, C. G. Townsend, H.-J. Miesner, D. S. Durfee, D. M. Kurn, and W. Ketterle, *Science* **275**, 637 (1997).
- [7] S. Inouye, S. Gupta, T. Rosenband, A. P. Chikkatur, A. Görlitz, T. L. Gustavson, A. E. Leanhardt, D. E. Pritchard, and W. Ketterle, *Phys. Rev. Lett.* **87**, 080402 (2001).
- [8] D. Jaksch, S. A. Gardiner, K. Schulze, J. I. Cirac, and P. Zoller, *Phys. Rev. Lett.* **86**, 4733 (2001).
- [9] K. Molmer, *Phys. Rev. A* **65**, 021607 (2002).
- [10] L. Pitaevskii and S. Stringari, *Phys. Rev. Lett.* **87**, 180402 (2001).
- [11] J. F. Corney, G. J. Milburn, and W. Zhang, *Phys. Rev. A* **59**, 4630 (1999).
- [12] J. Javanainen, *Phys. Rev. Lett.* **57**, 3164 (1986).
- [13] F. Dalfovo, L. Pitaevskii, and S. Stringari, *Phys. Rev. A* **54**, 4213 (1996).
- [14] G. J. Milburn, J. Corney, E. M. Wright, and D. F. Walls, *Phys. Rev. A* **55**, 4318 (1997).
- [15] I. Zapata, F. Sols, and A. J. Leggett, *Phys. Rev. A* **57**, R28 (1998).
- [16] A. Smerzi, S. Fantoni, S. Giovanazzi, and S. R. Shenoy, *Phys. Rev. Lett.* **79**, 4950 (1997).
- [17] J. E. Williams, *Phys. Rev. A* **64**, 013610 (2001).
- [18] C. Menotti, J. R. Anglin, J. I. Cirac, and P. Zoller, *Phys. Rev. A* **63**, 023601 (2001).
- [19] R. W. Spekkens and J. E. Sipe, *Phys. Rev. A* **59**, 3868 (1999).
- [20] Y. Kagan, E. L. Surkov, and G. V. Shlyapnikov, *Phys. Rev. A* **54**, R1753 (1996).
- [21] J. Javanainen and M. Y. Ivanov, *Phys. Rev. A* **60**, 2351 (1999).
- [22] P. Capuzzi and E. S. Hernández, *Phys. Rev. A* **59**, 3902 (1999).
- [23] B. Anderson and M. Kasevich, *Science* **282**, 1686 (1998).
- [24] C. Orzel, A. Tuchman, M. Fenselau, M. Yasuda, and M. Kasevich, *Science* **291**, 2386 (2001).
- [25] W. Hensinger *et al.*, *Nature (London)* **412**, 52 (2001).
- [26] S. Burger, F. S. Cataliotti, C. Fort, F. Minardi, M. Inguscio, M. L. Chiofalo, and M. P. Tosi, *Phys. Rev. Lett.* **86**, 4447 (2001).
- [27] F. S. Cataliotti, S. Burger, C. Fort, P. Maddaloni, F. Minardi, A. Trombettoni, A. Smerzi, and M. Inguscio, *Science* **293**, 843 (2001).
- [28] P. Pedri, L. Pitaevskii, S. Stringari, C. Fort, S. Burger, F. S. Cataliotti, P. Maddaloni, F. Minardi, and M. Inguscio, *Phys. Rev. Lett.* **87**, 220401 (2001).
- [29] O. Morsch, J. H. Müller, M. Cristiani, D. Ciampini, and E. Arimondo, *Phys. Rev. Lett.* **87**, 140402 (2001).
- [30] S. Burger, F. S. Cataliotti, C. Fort, P. Maddaloni, F. Minardi, and M. Inguscio, *Europhys. Lett.* **57**, 1 (2002).
- [31] M. Greiner, I. Bloch, O. Mandel, T. W. Hänsch, and T. Esslinger, *Phys. Rev. Lett.* **87**, 160405 (2001).
- [32] M. Greiner, O. Mandel, T. Esslinger, T. Hänsch, and I. Bloch, *Nature (London)* **415**, 39 (2002).
- [33] D. E. Pritchard, *Phys. Rev. Lett.* **51**, 1336 (1983).
- [34] T. Bergeman, G. Erez, and H. J. Metcalf, *Phys. Rev. A* **35**, 1535 (1987).
- [35] V. Boyer, S. Murdoch, Y. Le Coq, G. Delannoy, P. Bouyer, and A. Aspect, *Phys. Rev. A* **62**, 021601(R) (2000).
- [36] M.-O. Mewes, M. R. Andrews, N. J. van Druten, D. M. Kurn, D. S. Durfee, and W. Ketterle, *Phys. Rev. Lett.* **77**, 416 (1996).
- [37] E. A. Burt, R. W. Ghrist, C. J. Myatt, M. J. Holland, E. A. Cornell, and C. E. Wieman, *Phys. Rev. Lett.* **79**, 337 (1997).
- [38] C. A. Sackett, C. C. Bradley, M. Welling, and R. G. Hulet, *Appl. Phys. B: Photophys. Laser Chem.* **65**, 433 (1997).
- [39] L. V. Hau, B. D. Busch, C. Liu, Z. Dutton, M. M. Burns, and J. A. Golovchenko, *Phys. Rev. A* **58**, R54 (1998).
- [40] U. Ernst, A. Marte, F. Schreck, J. Schuster, and G. Rempe, *Europhys. Lett.* **41**, 1 (1998).
- [41] T. Esslinger, I. Bloch, and T. W. Hänsch, *Phys. Rev. A* **58**, R2664 (1998).
- [42] J. Söding, D. Guéry-Odelin, P. Desbiolles, F. Chevy, H. Inamori, and J. Dalibard, *Appl. Phys. B: Photophys. Laser Chem.* **69**, 257 (1999).
- [43] D. G. Fried, T. C. Killian, L. Willmann, D. Landhuis, S. C. Moss, D. Kleppner, and T. J. Greytak, *Phys. Rev. Lett.* **81**, 3811 (1998).
- [44] B. Desruelle, V. Boyer, S. G. Murdoch, G. Delannoy, P. Bouyer, A. Aspect, and M. Lécivain, *Phys. Rev. A* **60**, R1759 (1999).
- [45] R. Onofrio, D. S. Durfee, C. Raman, M. Köhl, C. E.

- Kuklewicz, and W. Ketterle, *Phys. Rev. Lett.* **84**, 810 (2000); R. Onofrio (private communication).
- [46] A. S. Arnold, C. McCormick, and M. G. Boshier, *Phys. Rev. A* **65**, 031601 (2002).
- [47] Y. Torii, Y. Suzuki, M. Kozuma, T. Sugiura, T. Kuga, L. Deng, and E. W. Hagley, *Phys. Rev. A* **61**, 041602 (2000).
- [48] C. Fort, M. Prevedelli, F. Minardi, F. S. Cataliotti, L. Ricci, G. M. Tino, and M. Inguscio, *Europhys. Lett.* **49**, 8 (2000).
- [49] A. Robert, O. Sirjean, A. Browaeys, J. Poupard, S. Nowak, D. Boiron, C. I. Westbrook, and A. Aspect, *Science* **292**, 461 (2001).
- [50] F. Pereira Dos Santos, J. Léonard, J. Wang, C. J. Barrelet, F. Perales, E. Rasel, C. S. Unnikrishnan, M. Leduc, and C. Cohen-Tannoudji, *Phys. Rev. Lett.* **86**, 3459 (2001).
- [51] A very similar double-well potential is used when loading laser-cooled atoms into a QUIC-style Ioffe-Pritchard trap [41].
- [52] W. Petrich, M. H. Anderson, J. R. Ensher, and E. A. Cornell, *Phys. Rev. Lett.* **74**, 3352 (1995).
- [53] K. B. Davis, M.-O. Mewes, M. A. Joffe, M. R. Andrews, and W. Ketterle, *Phys. Rev. Lett.* **74**, 5202 (1995).
- [54] M. Kozuma, L. Deng, E. W. Hagley, J. Wen, R. Lutwak, K. Helmerson, S. L. Rolston, and W. D. Phillips, *Phys. Rev. Lett.* **82**, 871 (1999).
- [55] J. H. Müller, D. Ciampini, O. Morsch, G. Smirne, M. Fazzi, P. Verkerk, F. Fuso, and E. Arimondo, *J. Phys. B* **33**, 4095 (2000).
- [56] J. R. Ensher, Ph.D. thesis, University of Colorado, Boulder, 1998, <http://jilawww.colorado.edu/www/sro/thesis/ensher/>
- [57] I. Bloch, T. W. Hänsch, and T. Esslinger, *Phys. Rev. Lett.* **82**, 3008 (1999).
- [58] J. Martin, C. McKenzie, N. Thomas, J. Sharpe, D. Warrington, P. Manson, W. Sandle, and A. Wilson, *J. Phys. B* **32**, 3065 (1999).
- [59] F. Dalfovo, S. Giorgini, L. P. Pitaevskii, and S. Stringari, *Rev. Mod. Phys.* **71**, 463 (1999).